Research Article

Double-Transmembrane Domain of SNAREs Decelerates the Fusion by Increasing the Protein-Lipid Mismatch

Bing Bu [1], Zhiqi Tian [2], Dechang Li [3*], Kai Zhang [4], Wei Chen [5], Baohua Ji [3] and Jiajie Diao [2*]

*1 - **Institute of Biomedical Engineering and Health Sciences,** Changzhou University, Changzhou, Jiangsu 213164, China*
*2 - **Department of Cancer Biology,** University of Cincinnati College of Medicine, Cincinnati, OH 45267, USA*
*3 - **Institute of Applied Mechanics,** Department of Engineering Mechanics, Zhejiang University, Hangzhou 310027, China*
*4 - **Department of Biochemistry,** University of Illinois, Urbana-Champaign, Illinois 61801, USA*
*5 - **Department of Cell Biology and Department of Cardiology of the Second Affiliated Hospital,** Zhejiang University School of Medicine, Zhejiang University, Hangzhou 310058, China*

***Correspondence to Dechang Li and Jiajie Diao:** dcli@zju.edu.cn (D. Li), jiajie.diao@uc.edu (J. Diao)*
https://doi.org/10.1016/j.jmb.2023.168089
Edited by Mingjie Zhang

Abstract

SNARE is the essential mediator of membrane fusion that highly relies on the molecular structure of SNAREs. For instance, the protein syntaxin-1 involved in neuronal SNAREs, has a single transmembrane domain (sTMD) leading to fast fusion, while the syntaxin 17 has a V-shape double TMDs (dTMDs), taking part in the autophagosome maturation. However, it is not clear how the TMD structure influences the fusion process. Here, we demonstrate that the dTMDs significantly reduce fusion rate compared with the sTMD by using an in vitro reconstitution system. Through theoretical analysis, we reveal that the V-shape dTMDs can significantly increase protein-lipid mismatch, thereby raising the energy barrier of the fusion, and that increasing the number of SNAREs can reduce the energy barrier or protein-lipid mismatch. This study provides a physicochemical mechanistic understanding of SNARE-regulated membrane fusion.

Introduction

As a key cellular process, membrane fusion plays a decisive role in neurotransmission, drug delivery, exocytosis and endocytosis.[1–4] Soluble N-ethylmaleimide-sensitive factor activating protein receptors (SNAREs) serve as the molecular machine to mediate neurotransmission and other fusion processes.[5–7] The core structure of neuronal SNAREs is composed of synaptobrevin-2 (Syb 2, also called VAMP2: vesicle-associated membrane protein 2), syntaxin-1 (Syx 1), and SNAP-25. The C-terminal single transmembrane domain (TMD) is one of the key structures of the SNAREs for membrane fusion. The TMD domain in Syb 2 is anchored on the synaptic vesicles, while Syx 1 is located in the plasma membrane. They wind with SNAP-25 and form a 4-helical SNARE core structure.[8] The extension of the zipper formation of the core structure to membranes by these two single TMDs is the main driving force of membrane fusion.[9] Most of the SNARE proteins have single TMD (sTMD); however, syntaxin 17 (Syx 17) serving in the fusion between autophagosomes and lysosomes contains the V-shape double TMDs (dTMDs)[7,10,11] (**Figure S1**). Defining the role of Syx 17 dTMDs in regulating membrane fusion is essential to the mechanistic understanding of the fusion machinery.

The TMD and its interaction with the membrane are determined by the lipids' physicochemical

properties and the TMD's structure.[1,12–17] For instance, Katsov et al.[12] suggested that lipids with spontaneous negative curvature, for example, phosphatidylethanolamine (PE) and cholesterol (Chol) have a lower energy barrier to fuse. Furthermore, Jackson considered the deformation and motion of the membrane and predicted the number and stiffness/flexibility of TMDs can regulate the fusion process and kinetics.[14,18] However, these studies mainly focused on either the SNAREs or the membrane individually, and the effect of SNAREs-lipid interaction on the fusion process is still unclear.

When the TMD domain of SNAREs (i.e. Syb and Syx) insert into the membrane, a protein-lipid mismatch may exist between the TMDs and the lipid bilayer due to the difference between the length of TMDs and the hydrophobic thickness of the lipid bilayer.[19–23] Such a protein-lipid mismatch can tilt the insertion angle of the TMDs depending on the length and sequence of TMDs and the membrane composition.[19–21] Therefore, this protein-lipid mismatch can change the interaction and local distribution of SNAREs and thus influence the fusion rate.[24,25] To date, however, few models consider the role of the SNAREs-lipid interaction in regulating the membrane fusion process. Effects of specific TMD configuration (e.g., sTMD versus dTMD) on membrane fusion are poorly understood.

We speculate that TMD configuration modifies SNAREs-lipid interaction and play a role in regulating membrane fusion. To test this hypothesis, instead of removing TMD as done in previous studies,[26] we compare the effect of sTMD and dTMD from syntaxin isoforms. Through ensemble lipid-mixing and single-vesicle docking assays, we found that the dTMDs of Syx 17 reduced the fusion rate about 4 times compared to the sTMD domain from the wildtype Syx 1 (Syx 1 WT). To explain this difference, we developed a model that treated the protein-lipid interaction explicitly and analyzed the effect of SNAREs-lipid mismatch on the membrane fusion. This model predicted that the increased protein-lipid mismatch by the dTMDs slowed the fusion process. We expect theoretical and experimental frameworks built in this study can be applied to study the regulatory roles of protein-lipid interaction involved in the membrane fusion process.

Materials and methods

Protein preparation

All SNARE proteins were from rat and expressed and purified as described by[27–29]. Briefly, his-tagged Syx 1A WT, Syx 1/17 containing the cytoplasmic domain of Syx 1A and the dTMDs of Sxy 17, and Syb 2 were expressed overnight at 25 °C in autoinducing media in *E. coli* strain C43. Cell pellets from 8 l of culture were suspended in 400 ml of 50 mM sodium phosphate pH 8.0, 1 M NaCl, 5 mM EDTA, and 1 mM PMSF supplemented with Complete Protease Inhibitor Cocktail tablets (Roche), and broken by three passes through an M-110-EH microfluidizer (Mircrofluidics Corp.) at 15,000 psi. After removing inclusion bodies, the membrane pellet was resuspended in 20 mM HEPES, pH 7.5, 1 mM *tris*(2-carboxyethyl)phosphine (TCEP), and 10 % (w/v) glycerol, and centrifuged for an additional 1 h in the same rotor. Membranes were suspended to a protein concentration of 5 mg/ml in buffer containing 20 mM HEPES, pH 7.5, 500 mM NaCl, 1 mM TCEP, 10 mM imidazole, and 10 % (w/v) glycerol, 1 mM PMSF supplemented with 2 EDTA-free Complete Protease Inhibitor Cocktail. Dodecylmaltoside (Anatrace) was added to 2 % (w/v), and after incubation at 4 °C for 1 h with stirring, the sample was centrifuged for 35 min at 40,000 rpm in a Ti-45 (Beckman Coulter) rotor, and the supernatant loaded onto a 1 ml column of Nickel-NTA agarose (Qiagen). Beads were harvested by centrifugation and poured into a column, attached to an AKTA Prime and washed with 50 ml of buffer containing 20 mM Hepes, pH 7.5, 300 mM NaCl, 1 mM TCEP, 20 mM imidazole, 110 mM OG and 10 % (w/v) glycerol, and the proteins were eluted in the same buffer containing 450 mM imidazole and 1 M NaCl. The protein-containing fractions were combined and injected on a Superdex 200 HR 10/300 GL (GE Healthcare) that was equilibrated with 20 mM Hepes, pH 7.5, 300 mM NaCl, 1 mM TCEP, 110 mM OG, and 10 % (w/v) glycerol. The peak fractions were then combined, and digested with 100 μg TEV protease that was removed by centrifugation at 5,000 rpm for 10 min. For SNAP-25, cysteine-free SNAP-25A (C84S, C85S, C90S, and C92S) was expressed from plasmid pTEV5 with an N-terminal TEV protease cleavable hexa-histidine tag. The proteins were expressed overnight at 25 °C in autoinducing media in *E. Coli* strain BL21(DE3). Cells from 4 L of culture were resuspended in 200 ml of 50 mM sodium phosphate, pH 8.0, 300 mM NaCl, and 20 mM imidazole supplemented with 1 mM PMSF and 4 EDTA-free protease inhibitor cocktail tablets. Cells were lysed by three passes through the Emulsiflex C5 homogenizer (Avestin) at 15,000 psi. The lysate was clarified by centrifugation in the Ti-45 rotor for 1.5 h at 40,000 rpm. The supernatant was bound to a 5 ml Nickel-NTA column by stirring at 4 °C for 1 hour. Beads with bound proteins were harvested by centrifugation, poured into a column and attached to an AKTA Prime (GE Healthcare). The column was washed with 150 ml of SNAP-25 buffer containing 50 mM sodium phosphate, pH 8.0, 300 mM NaCl supplemented with 50 mM imidazole and eluted with buffer containing 50 mM sodium phosphate, pH 8.0 and 300 mM NaCl supplemented with 350 mM imidazole. The protein containing fractions were combined, DTT was added to 5 mM, EDTA was added to 1 mM, and 150 μg of TEV protease was added to remove the hexa-histidine tag. This

mixture was dialyzed against buffer containing 20 mM HEPES, pH 7.5, 100 mM NaCl, and 4 mM DTT overnight at 4 °C. The TEV-cleaved SNAP-25 was concentrated in a 15 ml Amicon ultra centrifugal concentrator with a 10,000 molecular weight cutoff membrane (Millipore) to 5 ml and injected on the Superdex 200 (16/60) column (GE Healthcare) equilibrated with buffer containing 20 mM HEPES, pH 7.5, 100 mM NaCl, and 4 mM DTT.

Ensemble lipid mixing

A step-by-step protocol for v-/t-SNARE vesicle reconstitution for lipid mixing experiments has been reported in our previous publication.[30] The protein to lipid ratio was 1:200 for both t-SNARE and v-SNARE vesicles, by which approximately 100–200 copies of syx 1 or syb 2 proteins would be reconstituted to individual vesicles.[31,32] The lipid composition was 2:12:20:20:46 = DiI(DiD):PS:PE:Chol:PC. A 3- to 5-fold excess of SNAP-25 (with respect to syx 1) was added to the protein-lipid mixture for t-SNARE vesicles only. Detergent-free buffer (20 mM HEPES, pH 7.4, 90 mM NaCl, and 0.1% 2-mercaptoethanol) was added to the protein-lipid mixture until the detergent concentration was at the critical micelle concentration of 24.4 mM, *i.e.,* vesicle did not yet form. The vesicles subsequently formed during size exclusion chromatography using a Sepharose CL-4B column, that was equilibrated with buffer V (20 mM HEPES, pH 7.4, 90 mM NaCl) supplemented with 20 μM EGTA and 0.1% 2-mercaptoethanol. The eluent was subjected to dialysis into 2 L of detergent-free buffer V supplemented with supplemented with 20 μM EGTA, 0.1% 2-mercaptoethanol, 5 g of Bio-beads SM2 and 0.8 g/L Chelex 100 resin. After 4 h, the buffer was exchanged with 2 L of fresh buffer V containing 20 μM EGTA, 0.1% 2-mercaptoethanol and Bio-beads, and the dialysis continued for another 12 h.

DiI-labeled t-SNARE vesicles and DiD-labeled v-SNARE vesicles were mixed at a molar ratio of 1:1. To demonstrate the activity of vesicle fusion via lipid mixing, we measured acceptor fluorescence intensity by FRET using a fluorescence spectrometer (Varian Cary). Wavelengths of 530 and 670 nm were used for excitation of donor (DiI) and emission of acceptor (DiD), respectively. All experiments were performed at 35 °C.

Single vesicle docking

A detailed protocol for this step has been previously described.[33,34] The PEGylated surface of the microfluidic chamber was incubated with neutravidin (Invitrogen) for 5 min and washed with buffer V (20 mM HEPES, pH 7.4, 90 mM NaCl). The v-vesicles were immobilized on the surface with a 5-min incubation, and washed twice with 200 μL buffer V to remove free vesicles. Then, t-vesicles were injected and washed twice with 200 μL buffer V after 15 min of incubation. Docked t-vesicles were excited by a 532-nm laser (Crystal laser) on a total internal reflection fluorescence microscopy. The docking number per an imaging area ($45 \times 90\ \mu m^2$) was analyzed and averaged by using a customized program written in C++ (Microsoft).

Results

Effect of dTMDs on the fusion rate

To check the influence of dTMDs on fusion, we first performed experiments to investigate how the protein-lipid mismatch changes the fusion rate. Firstly, the dTMDs of Syx 17 were hybridized with Syx 1 WT (named as Syx 1/17) to eliminate the residue sequences difference of their zipping domains. We then performed an ensemble lipid-mixing assay to study the influence of dTMDs on the fusion process (Figure 1**(A)**). The fluorescence intensity produced by FRET between the donor and acceptor dyes in vesicles was measured for ~1800 s (Figure 1**(B)**). The same v-SNARE vesicles reconstituted with Syb 2 were used for vesicles reconstituted with Syx 1 WT (with sTMDs) and Syx 1/17 (with dTMDs). During the whole timecourse of fusion, the intensity of Syx 1 WT system is higher than that of Syx 1/17, indicating that the fusion rate of Syx 1 WT system is higher than that of Syx 1/17. By fitting the fluorescence intensity curve, we found that the fusion rate K of Syx 1 WT system is ~4.0 times as much as that of Syx 1/17. To eliminate the influence of dTMDs on vesicle docking, we also performed the single-vesicle docking assay (**Figure S2**). No difference on docking was observed (**Figure S2(B)**), indicating that replacing TMD of Syx 1 has little influence on the early stages of SNAREs zipping[35]; and the reduced lipid mixing lies on the fusion step. Moreover, since the vesicle docking is induced by the interaction of SNARE N-terminal domains, the result shown in **Figure S2(B)** also implies the reconstituted level of t-SNARE proteins for Syx 1 WT and Syx 1/17 vesicles was similar before TMDs comes to close contact[9] and the fusion reduction was mainly caused by the structural difference between dTMDs and sTMDs.

Theoretical estimation of fusion energy

A theoretical model was introduced to investigate the effect of protein-lipid mismatch between the length of TMDs and the membrane thickness on the membrane fusion. Three representative structures were used to capture the fusion process (Figure 2**(A)**).[36] In the beginning, the tilted TMDs of Syx and Syb formed bundles in the corresponding membranes (Figure 2**(A)**, α state); with the zipping of the SNAREs core helical structure, the TMDs rotated and moved along with the deformation of the membrane (Figure 2**(A)**, β state);

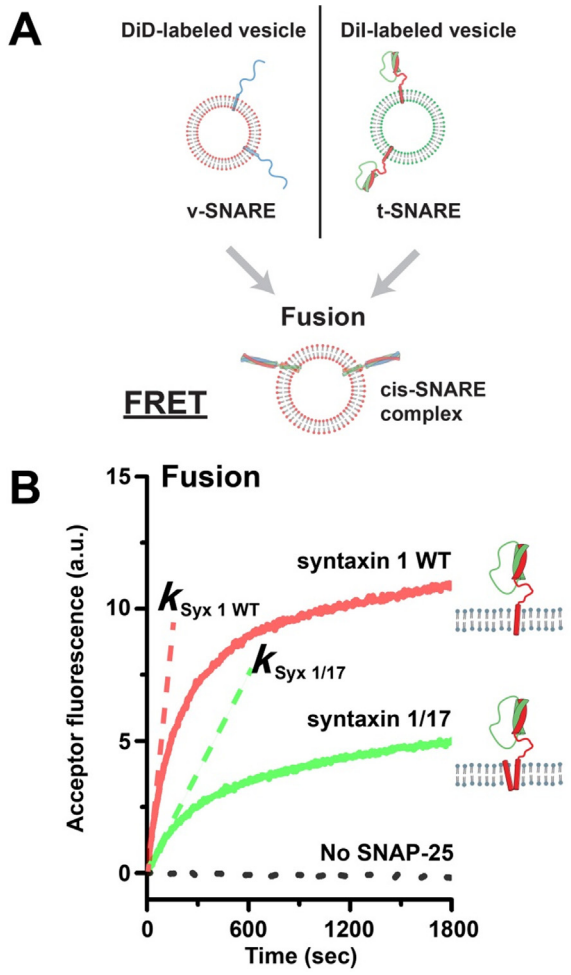

Figure 1. DTMDs reduce the rate of membrane fusion in vitro. (A) The illustration of v-vesicles and t-vesicles fusion. (B) Fusion of v-vesicles and t-vesicles reconstituted with syntaxin 1 wild-type (Syx 1 WT) with sTMDs and syntaxin 1 hybridized to the dTMDs of syntaxin 17 (Syx 1/17). The y axis is the acceptor fluorescence intensity produced by FRET between the donor and acceptor dyes in vesicles, a measure of the activity of vesicle fusion with lipid mixing. The acceptor fluorescence intensity of the experiment results in Figure 1**(B)** were analyzed by a high-order polynomial fitting (n = 9). The fusion rates are the slopes of the tangents of the acceptor fluorescence intensity curves at time t = 0, as the dash lines indicated.

when the SNARE zipping finished, the two opposed membranes merged and a fusion pore formed, the TMDs of Syx and Syb came to close contact (Figure 2**(A)**, γ state). In the theoretical model, we described the fusion process with a reaction coordinate d, the distance between the tails of transmembrane domain, as shown in the state β of Figure 2**(A)**. This distance is at its minimum, $d_{\min}$, at the state α; and it reaches its maximum, $d_{\max} = 2b$, after fusion at the state of γ, where b is the length of TMDs. Because d monotonically increases from α to γ state, we use its normalized form, $\xi(d) = (d - d_{\min})/(d_{\max} - d_{\min})$ as the fusion coordinate, to describe the fusion process. Note that $\xi(d) = 0$ at state α and $\xi(d) = 1$ at state γ. The membrane fusion process is mainly performed by SNAREs and lipid membranes. Inspired by a previous study,[14] we have three interaction/effect terms in fusion process: protein-lipid interaction, protein deformation and membrane deformation. Accordingly, the energy involved in the fusion process was divided into three parts

$$E = E_t + E_{Zipping} + E_{pore} \tag{1}$$

in which E_t is the energy induced by the protein-lipid mismatch; $E_{Zipping}$ is the energy released by the SNARE zipping, reflecting the protein deformation; and E_{pore} is the energy cost of the membrane deformation for forming a fusion pore, reflecting the membrane deformation.

The protein-lipid mismatch may exist due to the difference between the hydrophobic thickness of the lipid bilayer and the length of TMDs.[19–23] The transmembrane part of Syx 17 is usually combined tightly and exists as a double transmembrane domain.[10] Our model assumes no obvious protein–protein interaction change of the dTMDs during the fusion process. For TMDs with a positive or negative protein-lipid mismatch, the hydrophobic mismatch or rotation entropy will be induced when the TMDs insert into the membrane vertically[20,21,37] (Figure 2**(B)**). Thus, the TMDs prefer to insert into the membrane with a suitable tilt angle θ_t^s to accommodate the mismatch between TMDs and the lipid bilayer (Figure 2**(B)**).[20,21] Accordingly, the total interfacial energy depends on the tilt angle. Here we assume that the tile energy E_t changes linearly with number of the TMDs in the membrane during the fusion process (Figure 2**(A)** α to γ state), therefore the tilt energy is given by

$$E_t = N_t E_{t0}^{X\%} \xi(d) \tag{2}$$

where N_t is the number of TMDs involving in the fusion process. For single SNAREs complex, $N_t = 2$ (TMDs from Syx1 WT and Syb). For two SNAREs complex, $N_t = 4$ etc. $E_{t0}^{X\%}$ is the change of the tilt energy for one TMD during the fusion process. Previous studies[20,21] showed that the tilt energy $E_{t0}^{X\%}$ depends on the length of TMDs and the hydrophobic thickness of the membrane,[19,21,23] $X\%$ is a label for membrane composition contains $X\%$ Chol, which will be described later. As shown in Figure 2**(C)**, when the fusion process finishes (Figure 2**(A)**, γ state) and Syx comes to closely contact with Syb, both the TMDs insert in the membrane with a residual tilt angle θ_{t0} due to the radius of TMDs (Figure 2**(C)**). The radius of membrane contour curvature R_m (Figure 2**(C)**) was estimated in a range of 3–10 nm based on previous simulations and experiment results,[14,38–42] the radius of TMDs is $r = 0.35nm$.[14] Therefore, the residual tilt angle when the fusion process finishes can be calculated by $\theta_{t0} = \arcsin(r/R_m)$ (Figure 2**(C)**), and θ_{t0} comes to be $\sim 2.0 - 6.7°$. During the fusion process, the tilt

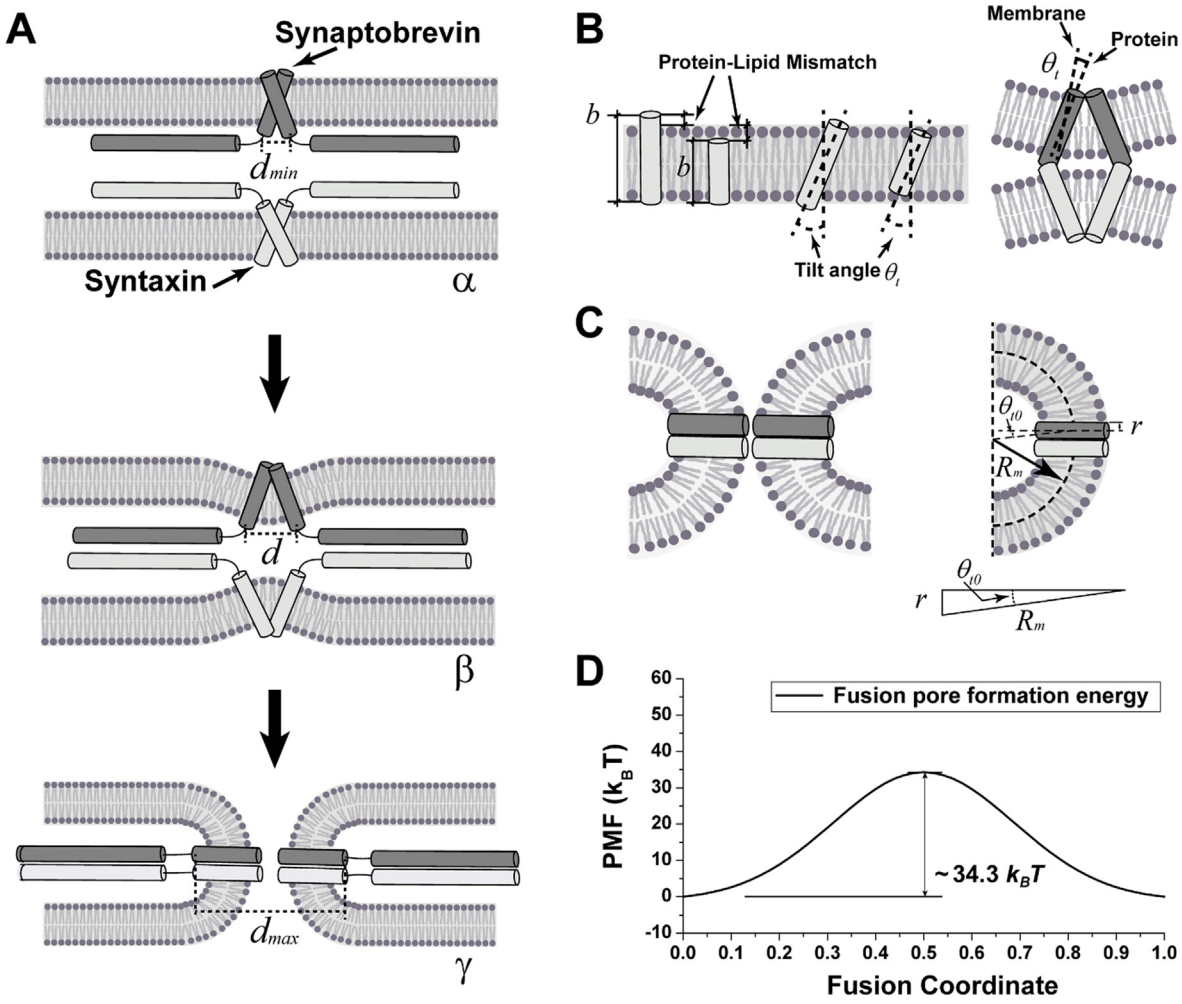

Figure 2. The fusion process with protein-lipid mismatch. (A) The representative structures of transition process from protein anchored in the membrane to fusion pore formation. TMDs rotated and moved, membrane deformed with fusion process from α to γ. $d_{\min}$, d, and $d_{\max}$ is the distance between the TMD's tails at different states, respectively. (B) The illustration of E_t energy contribution. E_t is the energy caused by the TMDs tilt (protein-lipid mismatch). b is the length of TMDs. θ_t is the tilt angle between the direction of TMDs and normal direction of membrane. (C) Illustration of protein-lipid mismatch interface in γ state. θ_{t0} is the residual tilt angle when the fusion process finished. R_m is the radius of curvature of membrane contour. r is the radius of TMD. The residual tilt angle θ_{t0} can be calculated as $\theta_{t0} = \arcsin(r/R_m)$. (D) The profile of fusion pore formation energy E_{pore} as a function of the fusion process was set as a Gauss curvature.[47]

angle changes from the suitable tilt angle θ_t^s to θ_{t0}. For a membrane with the hydrophobic thickness ~2.68 nm and the TMD length ~3.15 nm, the suitable title angle is $\theta_t^s = \sim 38.2^\circ$ and the tilt energy is $E_{t0}^{0\%} = \sim 2.3 - 4.4 k_B T$ according to the umbrella sampling calculations.[21]

Previous studies showed that the hydrophobic thickness of the membrane can be regulated by the proportion of Chol.[43,44] It was shown that Chol can increase the hydrophobic thickness of the membrane by ~0.32 nm with ~29% proportion, and the increase is almost linear to the Chol proportion.[43] The influence of Chol proportion on the hydrophobic thickness could be nonlinear. However, as shown by Drolle et al.,[43] the influence of Chol proportion on the thickness of the membrane containing DOPC could be approximately represented by a liner fitting. For a membrane with pure DOPC, the hydrophobic thickness is ~2.68 nm,[45] while the TMD of Syx contains 21 residues which has a length of ~3.15 nm. With a linear fitting, when the Chol proportion reaches to ~42.6%, the hydrophobic thickness of the membrane will be close to 3.15 nm, and the protein-lipid mismatch will be negligible. The Chol proportion will need to be about ~38.9% to lead to a 3.15 nm thickness membrane when using a quadratic fitting, comparable with the linear fitting result. To simplify the model, we use a simple linear fitting here. Note that although Chol can reduce the hydrophobic length mismatch between lipid and TMD, the tilt angle will

still exist even if the hydrophobic length mismatch is negligible.[21] For example, the TMD may have a $\sim 10^{\circ}$ inherent tilt angle and considerable helix rotation which arise from the helix precession around the membrane normal.[20,21,37] When the hydrophobic thickness of membrane is equal to the length of TMD, the tilt energy $E_{t0}^{X\%}$ is attributed to the rotational entropy contribution of the helix precession around the membrane normal, calculating as $E_{t0}^{X\%} = -k_B T \ln\left[\sin(\theta_{t0})/\sin\left(\theta_t^s\right)\right]$.[20,21,37] So that the change of the tilt energy with 42.6% Chol during the fusion process $E_{t0}^{42.6\%} = \sim 0.4 - 1.6 k_B T$ when the hydrophobic thickness of the membrane is equal to the length of TMD. We assumed that the tilt energy $E_{t0}^{X\%}$ depends on the Chol proportion linearly. So that for 20% Chol proportions, $E_{t0}^{X\%}$ comes to be $E_{t0}^{20\%} = \sim 1.4 - 3.1 k_B T$, respectively.

$E_{Zipping}$ is the energy of SNAREs zipping, which is assumed to be linear with $\xi(d)$

$$E_{zipping} = N \cdot E_0^{SNARE} \cdot \xi(d) \tag{3}$$

where $E_0^{SNARE} = 35 k_B T$ is the energy of each SNARE released during the fusion process.[46] As mentioned above, no difference in docking was observed with single and double TMDs (**Figure S2(B)**), indicating that extra TMD of Syx 17 has little influence on the protein–protein interaction and early stages of SNAREs zipping. The influence of extra TMD of Syx 1/17 is mainly reflected in the increase of protein-lipid mismatch.

Finally, E_{pore} is the energy cost for creating a fusion pore on the membrane during the fusion process. The membrane deformation during the fusion process should pass several metastable states and overcome energy barriers for, e.g., stalk, hemifusion, and fusion pore formation. These energy barriers can be represented by one effective energy barrier[47] and simplified as a Gaussian-like form.[48] The energy profile changing with the fusion coordinate is fitted with an energy barrier of $E_b^{pore} = 34.3 k_B T$ [47] as

$$E_{pore} = y_0 + E_0^{pore} e^{-\frac{\left(\xi(d)-\frac{1}{2}\right)^2}{2\omega^2}} \tag{4}$$

The parameters used in this study are listed in Table 1.

To calculate the fusion rate with the Kramers' theory,[14,49,50] the reaction rate k can be written as[14]

$$k = \frac{\sqrt{\phi_{well} \cdot \phi_{barrier}}}{f} e^{-\Delta E / k_B T} \tag{5}$$

where ΔE is the energy barrier of the reaction. ϕ_{well} and $\phi_{barrier}$ are the quadratic coefficients for the energy profile at the minimum and at the peak of the barrier, respectively. f is a constant related to the diffusion coefficient. k_B is the Boltzmann constant, and T is the absolute temperature. Finally, we got the ratio of the fusion rate between two reactions of i and j

$$\frac{k_i}{k_j} = \frac{\sqrt{\phi_{well}^i \cdot \phi_{barrier}^i}}{\sqrt{\phi_{well}^j \cdot \phi_{barrier}^j}} e^{-\left(\Delta E^i - \Delta E^j\right)/k_B T} \tag{6}$$

Effect of protein-lipid mismatch

The total energy of membrane fusion was calculated for different numbers of SNAREs. The energy profiles and energy barrier for N = 1∼3 are shown in Figure 3**(A)**. Our data show that the energy barriers decrease with the increasing number of SNAREs taking part in the fusion process. When N = 3, the energy barrier for the fusion nearly vanishes (see Figure 3**(A)**). These data suggest that the fusion is highly accelerated when more SNAREs are involved, consistent with a previous study showing that efficient fusion requires three or more SNARE complexes.[51]

To investigate the influence of protein-lipid mismatch between the TMDs and lipid bilayer on the fusion process, we calculated the energy profile with two SNAREs during fusion in the presence and absence of protein-lipid mismatch. The energy barrier of the fusion process in the presence of protein-lipid mismatch is $\sim 2.4 k_B T$ higher (Figure 3**(B)**). At the beginning of the protein-lipid-mismatch fusion, the TMDs are tilted in the membrane (see α state in Figure 2**(A)**). After the formation of the fusion pore, the TMDs of Syb and Syx contact with each other and are almost perpendicular to the membrane (see γ state in Figure 2**(A)** and Figure 2**(C)**). It is clearly suggested that the increase of energy barrier is caused by the protein-lipid mismatch. Thus, the fusion process with the protein-lipid mismatch experiences a higher energy barrier, leading to a slower fusion rate.

Table 1 The definitions and parameters for the theoretical model.

Symbol	Definition	Values	Ref
N	Number of SNARE complexes	1–3	51
r	Radius of TMDs	3.5 Å	14
R_m	Radius of membrane contour curvature	3–10 nm	14,38–42
$E_{t0}^{0\%}$	Tilt energy change during fusion process with 0% Chol	$\sim 2.3 - 4.4 k_B T$	21
E_b^{pore}	Energy to generate a membrane fusion pore	$34.3 k_B T$	47
y_0	Gauss curvature parameter	$-1.01 k_B T$	Fitting with[47]
E_0^{pore}	Gauss curvature parameter	$35.3 k_B T$	Fitting with[47]
ω	Gauss curvature parameter	0.188	Fitting with[47]
E_{SNARE}	Energy provided by one SNARE protein	$35 k_B T$	46

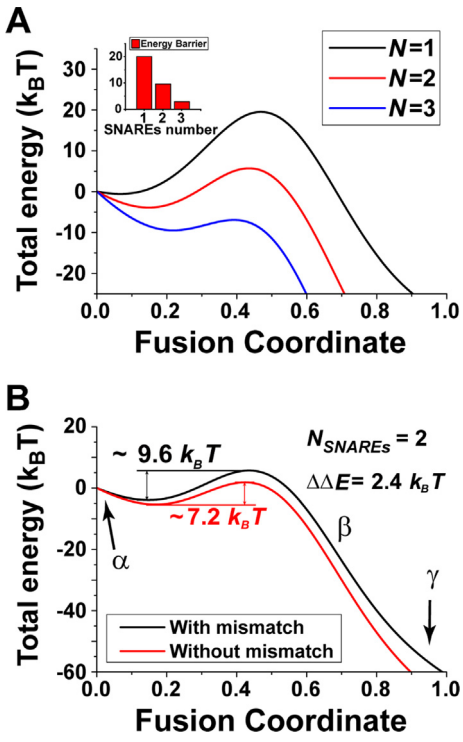

Figure 3. (A) The fusion energy profiles and barrier changed with different SNAREs number. (B) The energy profile of fusion process with and without mismatch as a function of fusion coordinate. Two SNAREs were assumed to take part in the fusion process. To consistent with the experiment, the $E_{t0} = 2.25k_BT$ was used in the theoretical claculation with 20% Chol.

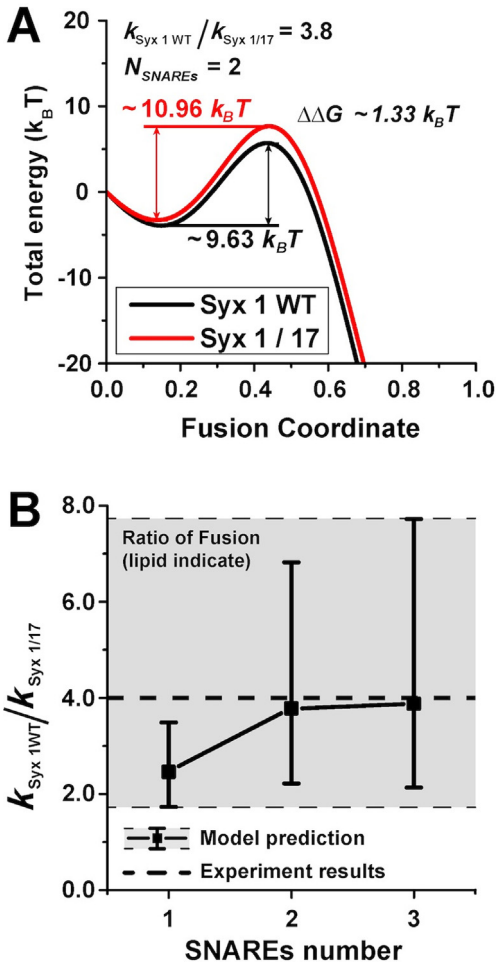

Figure 4. Theoretic analysis of fusion behaviors of systems with Syx 1 WT and Syx 1/17. (A) The energy profiles of Syx 1 WT and Syx 1/17 as function of fusion coordinate. Two SNAREs were assumed to take part in the fusion process. (B) The ratio of fusion rate between Syx 1 WT and Syx 1/17 with various SNAREs number predicted by the theoretical model that was compared with the experiment results. The solid line with square symbol illustrates that tilt energy $E_{t0} = 2.25k_BT$ (20% Chol) and SNAREs number varies from 1 to 3. The experimental result $k_{Syx\ 1\ WT}/k_{Syx\ 1/17}$ is obtained by a high-order polynomial fitting (n = 9) of the experimental curvature in Figure 1**(B)**. The light grey shadow region illustrates that tilt energy E_{t0} varies from 1.4 to $3.1k_BT$ (20% Chol) and the number of SNAREs varies from 1 to 3.

Effect of SNARE number

To further understand our experimental results showing double-TMDs reduce fusion (Figure 1), we analyzed the influence of dTMDs with our theoretical model. The change of the tilt energy during the fusion process with dTMDs is larger than that with sTMD because of the increase of TMD numbers N_t. The difference in the geometric arrangement of TMDs and their interaction with lipid bilayer between the systems with sTMD and dTMDs is illustrated in **Figure S3**. The energy profile during the fusion process is shown in Figure 4**(A)**. When 1–3 SNAREs were involved in the fusion process, the fusion rate of Syx 1 WT could be ~1.7–7.7 times higher than that of Syx 1/17 (Figure 4**(B)**). For example, when two SNAREs take part in the fusion process, the dTMDs increase the fusion energy barrier and reduces the fusion rate. The energy barrier of Syx 1/17 is $\sim 1.33k_BT$ higher than that of Syx 1 WT, so that the fusion rate of Syx1 WT is ~3.8 times higher than that of Syx 1/17, consistent with the experimental results (Figure 1**(B)**). Note that various experiment methods get different SNAREs energy E_0^{SNARE}, it is $\sim 68 - 85k_BT$ with magnetic and optical tweezers.[35,52] Besides, the estimates obtained with atomic-force microscopy or the surface-force apparatus are much lower, which was in the $30k_BT$ range.[46,52] Li et al. suggested that SNAREs release $E_0^{SNARE} = 35 \pm 7k_BT$.[46] Considering the error effect of E_0^{SNARE}, we calculated $k_{Syx\ 1\ WT}/k_{Syx\ 1/17}$ when E_0^{SNARE} varies from 28 to $42k_BT$ with tilt energy $E_{t0} = 2.25k_BT$ (20% Chol). When $E_0^{SNARE} = 28k_BT$, the fusion rate of Syx 1 WT could be ~2.6–6.2 times higher than that of

Syx 1/17; when $E_0^{SNARE} = 35k_BT$, the fusion rate of Syx 1 WT could be ~2.5–3.9 times higher than that of Syx 1/17; when $E_0^{SNARE} = 42k_BT$, the fusion rate of Syx 1 WT could be ~2.3–3.9 times higher than that of Syx 1/17. Both our experimental and theoretical results show that the dTMDs reduce fusion rate significantly, which can be explained why the fusion process of autophagosomes and lysosomes is slower than the fusion in neurotransmission.[26,53] In addition, our results suggest that the number of SNAREs involved in a general fusion process is likely to be 2 to 3 (see Figure 4**(B)**).

Discussion and conclusions

The interplay between the protein and membrane is essential for membrane fusion.[54] As the direct link between SNAREs and the membrane, TMD attracts significant interest in biophysical and biochemical research of SNARE-mediated membrane fusion.[55,56] Here in this study, we studied how the structure of TMD influenced the fusion rate with the development of a unique technique of adding an extra TMD in the protein. We showed that the dTMDs led to a slower membrane fusion rate compared with the sTMD. The mechanism is that the dTMDs induced a larger protein-lipid mismatch. Both of our experimental and theoretical results showed that the protein-lipid mismatch could significantly increase the energy barrier for membrane fusion and thus reduces the fusion rate.

Furthermore, we analyzed how the number of SNAREs influences the fusion rate. The SNARE number involved in a fusion process is a hotspot in the fusion-related research.[14,51,57–60] The controversy regarding the number still exists in the field, and the proposed number range from one to some dozens.[58] Our results showed that 2–3 SNAREs are more likely involved in a general fusion process, consistent with previous studies[51,58–60] that reported that one to three SNAREs are sufficient for completing the membrane fusion.[51,60] This study provides a quantitative understanding on the effect of the structure of SNAREs on the regulation of membrane fusion.

CRediT authorship contribution statement

Bing Bu: Methodology, Validation, Data curation, Writing – original draft. **Zhiqi Tian:** Methodology, Validation, Data curation. **Dechang Li:** Conceptualization, Project administration, Supervision, Investigation, Writing – review & editing. **Kai Zhang:** Supervision, Resources, Writing – review & editing. **Wei Chen:** Supervision, Resources, Writing – review & editing. **Baohua Ji:** Supervision, Resources, Writing – review & editing. **Jiajie Diao:** Funding acquisition, Conceptualization, Project administration, Supervision, Investigation, Writing – review & editing.

Acknowledgments

The authors would like to thank Mark Padolina in Axel Brunger's Lab at Stanford University for protein preparation. K.Z. was supported by the School of Molecular Cell Biology at the University of Illinois at Urbana-Champaign. J.D. was supported by the NIH (R35GM128837).

Author Contributions

D.L., B.J., and J.D. contributed to concept and design of this study. B.B. performed theoretical calculation. Z.T. performed and analyzed data for fusion and docking experiments. B.B., D.L., K.Z., W.C., B.J., and J.D. wrote manuscript.

Declaration of Competing Interest

The authors declare that they have no known competing financial interests or personal relationships that could have appeared to influence the work reported in this paper.

Appendix A. Supplementary Data

Supplementary data to this article can be found online at https://doi.org/10.1016/j.jmb.2023.168089.

Received 1 March 2023;
Accepted 2 April 2023;
Available online 7 April 2023

Keywords:
membrane fusion;
transmembrane domain;
protein-lipid mismatch

References

1. Chernomordik, L.V., Kozlov, M.M., (2008). Mechanics of membrane fusion. *Nat. Struct. Mol. Biol.* **15**, 675–683.
2. Cho, S., von Gersdorff, H., (2013). Neuroscience: Faster than kiss-and-run. *Nature* **504**, 220–221.
3. Fuhrmans, M., Marelli, G., Smirnova, Y.G., Muller, M., (2015). Mechanics of membrane fusion/pore formation. *Chem. Phys. Lipids* **185**, 109–128.
4. Jahn, R., Scheller, R.H., (2006). SNAREs–engines for membrane fusion. *Nat. Rev. Mol. Cell Biol.* **7**, 631–643.
5. Chen, Y.A., Scheller, R.H., (2001). SNARE-mediated membrane fusion. *Nat. Rev. Mol. Cell Biol.* **2**, 98–106.
6. Wang, Y., Li, L., Hou, C., Lai, Y., Long, J., Liu, J., et al., (2016). SNARE-mediated membrane fusion in autophagy. *Semin. Cell Dev. Biol.* **60**, 97–104.
7. Chen, Q., Hao, M., Wang, L., Li, L., Chen, Y., Shao, X., et al., (2021). Prefused lysosomes cluster on

autophagosomes regulated by VAMP8. *Cell Death Dis.* **12**, 939.
8. Sutton, R.B., Fasshauer, D., Jahn, R., Brunger, A.T., (1998). Crystal structure of a SNARE complex involved in synaptic exocytosis at 2.4 angstrom resolution. *Nature* **395**, 347–353.
9. Stein, A., Weber, G., Wahl, M.C., Jahn, R., (2009). Helical extension of the neuronal SNARE complex into the membrane. *Nature* **460**, 525–528.
10. Itakura, E., Kishi-Itakura, C., Mizushima, N., (2012). The hairpin-type tail-anchored SNARE syntaxin 17 targets to autophagosomes for fusion with endosomes/lysosomes. *Cell* **151**, 1256–1269.
11. Itakura, E., Mizushima, N., (2013). Syntaxin 17: the autophagosomal SNARE. *Autophagy* **9**, 917–919.
12. Katsov, K., Muller, M., Schick, M., (2004). Field theoretic study of bilayer membrane fusion. I. Hemifusion mechanism. *Biophys. J.* **87**, 3277–3290.
13. Jackson, M.B., (2009). Minimum membrane bending energies of fusion pores. *J. Membr. Biol.* **231**, 101–115.
14. Jackson, M.B., (2010). SNARE complex zipping as a driving force in the dilation of proteinaceous fusion pores. *J. Membr. Biol.* **235**, 89–100.
15. Ryham, R.J., Klotz, T.S., Yao, L., Cohen, F.S., (2016). Calculating Transition Energy Barriers and Characterizing Activation States for Steps of Fusion. *Biophys. J.* **110**, 1110–1124.
16. Mostafavi, H., Thiyagarajan, S., Stratton, B.S., Karatekin, E., Warner, J.M., Rothman, J.E., et al., (2017). Entropic forces drive self-organization and membrane fusion by SNARE proteins. *PNAS* **114**, 5455–5460.
17. Bu, B., Tian, Z., Li, D., Ji, B., (2016). High Transmembrane Voltage Raised by Close Contact Initiates Fusion Pore. *Front. Mol. Neurosci.* **9**, 1–10.
18. Dhara, M., Mantero Martinez, M., Makke, M., Schwarz, Y., Mohrmann, R., Bruns, D., (2020). Synergistic actions of v-SNARE transmembrane domains and membrane-curvature modifying lipids in neurotransmitter release. *Elife* **9**, e55152
19. Strandberg, E., Esteban-Martin, S., Ulrich, A.S., Salgado, J., (2012). Hydrophobic mismatch of mobile transmembrane helices: Merging theory and experiments. *Biochim. Biophys. Acta* **1818**, 1242–1249.
20. Lee, J., Im, W., (2008). Transmembrane helix tilting: insights from calculating the potential of mean force. *Phys. Rev. Lett.* **100**, 018103
21. Kim, T., Im, W., (2010). Revisiting hydrophobic mismatch with free energy simulation studies of transmembrane helix tilt and rotation. *Biophys. J.* **99**, 175–183.
22. Bowen, M., Brunger, A.T., (2006). Conformation of the synaptobrevin transmembrane domain. *PNAS* **103**, 8378–8383.
23. Blanchard, A.E., Arcario, M.J., Schulten, K., Tajkhorshid, E., (2014). A highly tilted membrane configuration for the prefusion state of synaptobrevin. *Biophys. J.* **107**, 2112–2121.
24. Milovanovic, D., Honigmann, A., Koike, S., Gottfert, F., Pahler, G., Junius, M., et al., (2015). Hydrophobic mismatch sorts SNARE proteins into distinct membrane domains. *Nat. Commun.* **6**, 5984.
25. Killian, J.A., (1998). Hydrophobic mismatch between proteins and lipids in membranes. *Bba-Rev. Biomembranes.* **1376**, 401–416.
26. Zhou, P., Bacaj, T., Yang, X., Pang, Z.P., Sudhof, T.C., (2013). Lipid-anchored SNAREs lacking transmembrane regions fully support membrane fusion during neurotransmitter release. *Neuron* **80**, 470–483.
27. Gong, J., Lai, Y., Li, X., Wang, M., Leitz, J., Hu, Y., et al., (2016). C-terminal domain of mammalian complexin-1 localizes to highly curved membranes. *PNAS* **113** E7590-E9.
28. Lai, Y., Choi, U.B., Zhang, Y., Zhao, M., Pfuetzner, R.A., Wang, A.L., et al., (2016). N-terminal domain of complexin independently activates calcium-triggered fusion. *PNAS* **113** E4698-707.
29. Lai, Y., Diao, J.J., Cipriano, D.J., Zhang, Y.X., Pfuetzner, R.A., Padolina, M.S., et al., (2014). Complexin inhibits spontaneous release and synchronizes Ca2+-triggered synaptic vesicle fusion by distinct mechanisms. *Elife* **3**, e03756.
30. Diao, J., Li, L., Lai, Y., Zhong, Q., (2017). In Vitro Reconstitution of Autophagosome-Lysosome Fusion. *Methods Enzymol.* **587**, 365–376.
31. Diao, J., Ishitsuka, Y., Lee, H., Joo, C., Su, Z.L., Syed, S., et al., (2012). A single vesicle-vesicle fusion assay for in vitro studies of SNAREs and accessory proteins. *Nat. Protoc.* **7**, 921–934.
32. Kyoung, M.J., Zhang, Y.X., Diao, J.J., Chu, S., Brunger, A. T., (2013). Studying calcium-triggered vesicle fusion in a single vesicle-vesicle content and lipid-mixing system. *Nat. Protoc.* **8**, 1–16.
33. Diao, J., Cipriano, D.J., Zhao, M., Zhang, Y., Shah, S., Padolina, M.S., et al., (2013). Complexin-1 enhances the on-rate of vesicle docking via simultaneous SNARE and membrane interactions. *J. Am. Chem. Soc.* **135**, 15274–15277.
34. Diao, J., Yoon, T.Y., Su, Z., Shin, Y.K., Ha, T., (2009). C2AB: a molecular glue for lipid vesicles with a negatively charged surface. *Langmuir : ACS J. Surf. Colloids* **25**, 7177–7180.
35. Zhang, Y., Ma, L., Bao, H., (2022). Energetics, kinetics, and pathways of SNARE assembly in membrane fusion. *Crit. Rev. Biochem. Mol. Biol.57*, 443–460.
36. Han, J., Pluhackova, K., Bockmann, R.A., (2017). The Multifaceted Role of SNARE Proteins in Membrane Fusion. *Front. Physiol.* **8**, 5.
37. Lee, J., Im, W., (2007). Restraint potential and free energy decomposition formalism for helical tilting. *Chem. Phys. Lett.* **441**, 132–135.
38. Diao, J., Grob, P., Cipriano, D.J., Kyoung, M., Zhang, Y., Shah, S., et al., (2012). Synaptic proteins promote calcium-triggered fast transition from point contact to full fusion. *Elife* **1**, e00109.
39. Bu, B., Crowe, M., Diao, J., Ji, B., Li, D., (2018). Cholesterol suppresses membrane leakage by decreasing water penetrability. *Soft Matter* **14**, 5277–5282.
40. Tsai, H.H., Chang, C.M., Lee, J.B., (2014). Multi-step formation of a hemifusion diaphragm for vesicle fusion revealed by all-atom molecular dynamics simulations. *Biochim. Biophys. Acta* **1838**, 1529–1535.
41. Kawamoto, S., Klein, M.L., Shinoda, W., (2015). Coarse-grained molecular dynamics study of membrane fusion: Curvature effects on free energy barriers along the stalk mechanism. *J. Chem. Phys.* **143**, 243112
42. Lai, Y., Zhao, L., Bu, B., Lou, X., Li, D., Ji, B., et al., (2015). Lipid molecules influence early stages of yeast SNARE-mediated membrane fusion. *Phys. Biol.* **12**, 025003

43. Drolle, E., Kucerka, N., Hoopes, M.I., Choi, Y., Katsaras, J., Karttunen, M., et al., (2013). Effect of melatonin and cholesterol on the structure of DOPC and DPPC membranes. *Biochim. Biophys. Acta* **1828**, 2247–2254.
44. Yang, S.T., Kreutzberger, A.J.B., Lee, J., Kiessling, V., Tamm, L.K., (2016). The role of cholesterol in membrane fusion. *Chem. Phys. Lipids* **199**, 136–143.
45. Guo, Y., Pogodin, S., Baulin, V.A., (2014). General model of phospholipid bilayers in fluid phase within the single chain mean field theory. *J. Chem. Phys.* **140**, 174903
46. Li, F., Pincet, F., Perez, E., Eng, W.S., Melia, T.J., Rothman, J.E., et al., (2007). Energetics and dynamics of SNAREpin folding across lipid bilayers. *Nat. Struct. Mol. Biol.* **14**, 890–896.
47. Francois-Martin, C., Rothman, J.E., Pincet, F., (2017). Low energy cost for optimal speed and control of membrane fusion. *PNAS* **114**, 1238–1241.
48. Manca, F., Pincet, F., Truskinovsky, L., Rothman, J.E., Foret, L., Caruel, M., (2019). SNARE machinery is optimized for ultrafast fusion. *PNAS* **116**, 2435–2442.
49. Hänggi, P., Talkner, P., Borkovec, M., (1990). Reaction-rate theory: fifty years after Kramers. *Rev. Mod. Phys.* **62**, 251–341.
50. Kramers, H.A., (1940). Brownian motion in a field of force and the diffusion model of chemical reactions. *Physica* **7**, 284–304.
51. Shi, L., Shen, Q.T., Kiel, A., Wang, J., Wang, H.W., Melia, T.J., et al., (2012). SNARE proteins: one to fuse and three to keep the nascent fusion pore open. *Science* **335**, 1355–1359.
52. Rizo, J., Xu, J., (2015). The Synaptic Vesicle Release Machinery. *Annu. Rev. Biophys.* **44**, 339–367.
53. Watanabe, S., Rost, B.R., Camacho-Perez, M., Davis, M. W., Sohl-Kielczynski, B., Rosenmund, C., et al., (2013). Ultrafast endocytosis at mouse hippocampal synapses. *Nature* **504**, 242–247.
54. van den Bogaart, G., Meyenberg, K., Risselada, H.J., Amin, H., Willig, K.I., Hubrich, B.E., et al., (2011). Membrane protein sequestering by ionic protein-lipid interactions. *Nature* **479**, 552–555.
55. Tian, Z., Gong, J., Crowe, M., Lei, M., Li, D., Ji, B., et al., (2019). Biochemical studies of membrane fusion at the single-particle level. *Prog. Lipid Res.* **73**, 92–100.
56. Bao, H., Das, D., Courtney, N.A., Jiang, Y., Briguglio, J.S., Lou, X., et al., (2018). Dynamics and number of trans-SNARE complexes determine nascent fusion pore properties. *Nature* **554**, 260–263.
57. Karatekin, E., Di Giovanni, J., Iborra, C., Coleman, J., O'Shaughnessy, B., Seagar, M., et al., (2010). A fast, single-vesicle fusion assay mimics physiological SNARE requirements. *PNAS* **107**, 3517–3521.
58. Xu, W., Nathwani, B., Lin, C., Wang, J., Karatekin, E., Pincet, F., et al., (2016). A Programmable DNA Origami Platform to Organize SNAREs for Membrane Fusion. *J. Am. Chem. Soc.* **138**, 4439–4447.
59. van den Bogaart, G., Holt, M.G., Bunt, G., Riedel, D., Wouters, F.S., Jahn, R., (2010). One SNARE complex is sufficient for membrane fusion. *Nat. Struct. Mol. Biol.* **17**, 358–364.
60. Sinha, R., Ahmed, S., Jahn, R., Klingauf, J., (2011). Two synaptobrevin molecules are sufficient for vesicle fusion in central nervous system synapses. *PNAS* **108**, 14318–14323.